

# A Method to Characterize the Mechanical Behavior of Human Soft Tissue Using Finite Element Analysis

M. Schrodtt<sup>a,b</sup> G. Benderoth<sup>a,b</sup> M. Alizadeh<sup>d</sup> J. Menger<sup>a,b</sup>  
T. Vogl<sup>c</sup> G. Silber<sup>a,b,\*</sup>

<sup>a</sup>*Center of Biomedical Engineering (CBME), Frankfurt/M.*

<sup>b</sup>*Institute for Materials Science, University of Applied Sciences Frankfurt,  
Nibelungenplatz 1 D-60318 Frankfurt*

<sup>c</sup>*Department of Diagnostic and Interventional Radiology, Hospital of the Johann  
Wolfgang Goethe University Frankfurt/M, Theodor-Stern-Kai 7 D-60590 Frankfurt  
am Main*

<sup>d</sup>*University of Science & Technology, Teheran (Iran)*

---

## Abstract

In order to analyze the mechanical aspects of such diseases like decubitus ulcer an analysis of the mechanical behavior and interaction of various human body parts is necessary. Because of the complexity of the problem an FE analysis is an appropriate method. But this analysis can only be carried out, if there is an adequate mechanical description of human soft tissues. So this analysis deals with the mechanical description of these tissues.

Because of the hydraulic nature of human soft tissue, its mechanical behavior depends strongly on its filling condition. Thus mechanical properties of tissue have to be measured while part of the whole organism to guarantee reproducible filling conditions.

In order to characterize the tissue a testing device was constructed to conduct loading experiments on parts of the body. The geometry of such a body part under deformation was grabbed in a MRI device. The images were used to generate a three dimensional FE model. By using this model and the data from the loading test a parameter identification for a hyperelastic constitutive law was carried out. This was done with a non linear optimization tool using an FE tool as a solver of the quality function.

It could be shown that for the hyperelastic constitutive law introduced by OGDEN a successful identification could be carried out. This method can be applied to different constitutive laws and various tissue measuring sites.

*Key words:* mechanical properties, human soft tissue, hyperelasticity, slightly

---

\* Corresponding author

*Email address:* `silber@fb2.fh-frankfurt.de` (G. Silber).

## 1 Introduction

The mechanical properties of soft tissue are involved in various human diseases. So e.g. malignant tissue eliminates healthy tissue by applying higher cellular pressure, or decubitus ulcers are induced by applying a continuous pressure on the skin of a person. If one wants to evaluate the influence of the mechanic load on such diseases, one has to describe the mechanical properties of soft tissue adequately and investigate the interaction of soft tissue within the human body with characteristic loads which are partly responsible for the occurrence of such diseases. This analysis is a contribution to this process.

To characterize the mechanical behavior of soft tissue one needs suitable experiments, a theoretical description of its behavior and a procedure to determine the parameters of the mechanical model.

There are quite a few empirical studies which have investigated the mechanical behavior of soft tissue. Such studies range from investigation of isolated parts of soft tissue *ex vivo* (as e.g. in Miller and Chinzei (1997), Daly et al. (2000) or in Samani and Plewes (2004), Sacks (2000) and Miller et al. (2002)) through *ex vivo* studies of whole soft tissue structures like a muscular fascia (as in Maenhout et al. (2000) and Palevski et al. (2006)) up to the deformation reconstruction of a whole collection of soft tissues of dead bodies using imaging procedures (Moes and Horvath, 2002). The method chosen for this study is also an imaging procedure for investigating the deformation of a whole compound of soft tissues. The chosen method was MRI because the representation of soft tissue shows the best results with this method. Unlike to Moes and Horvath (2002) the deformation experiment was performed on a compound of soft tissue of a living person. This scenario was chosen because the filling condition of different soft tissue influences the mechanical response of the tissue to loading quite significantly.

Experimental results (see e.g. Daly et al. (2000)) indicate that the mechanical behavior of the tissue can be modeled with a hyperelastic constitutive equation. Often used is the constitutive equation introduced by Mooney and Ogden (1972) (see e.g. Daly et al. (2000), Miller et al. (2002) and Samani and Plewes (2004)). For this study an Ogden type constitutive equation was used, because good results for the parameter optimization had been obtained with this model.

To determine the parameters within the Ogden law, a non linear optimization routine has to be used. The routine used in this study is the *Simplex* algorithm presented by Nelder and Mead (1969). Because of the complexity of the geometry of the loaded tissue, the quality function of the optimization algorithm has to be evaluated using an FE program.

## 2 Mechanical assumption about human soft tissue

Human soft tissue consists of a viscoelastic fill and membranous cover made of a woven mesh of protein fibres. Such a cover acts like a membrane, which means that it is limp and can only be loaded through tensile and not through compression stresses. Furthermore the membrane is permeable for small molecules like water and some ions. Figure 1 demonstrates one effect of the response of such a construction to mechanical loads. If the fill does not occupy the total possible volume of the cover (left hand side of figure 1), this fill is displaced inside the cover by the load as long as the enclosed volume of the cover fits with the volume of the fill, almost without causing a load signal. So the filling status of the system influences the mechanical behavior considerably (compare Figure 1). Due to the water permeability of the membrane, each loading causes a loss of volume of the fill.

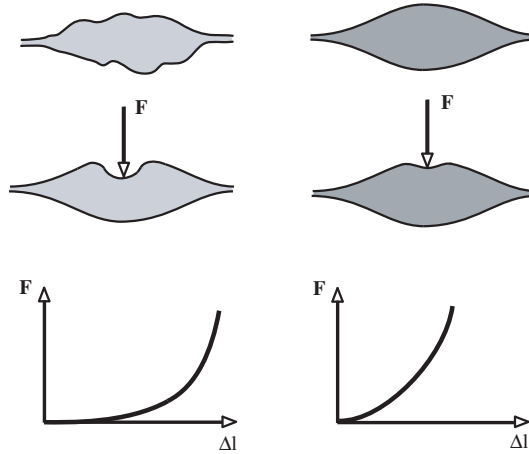


Fig. 1. A cover fill system not affected by gravity. On the left side the cover is underfilled with a viscoelastic fill whereas on the right side the volume of the fill equals the volume of the cover.

## 3 Experiment

The standard procedure for determining the mechanical properties of materials is to choose an adequate constitutive model, perform a loading experiment and determine the model parameters in such a way that the model represents the experimental data.

**Experimental set up:** As mentioned in the introduction there are various approaches to conduct appropriate experiments. For this analysis an in vivo experimental scenario was chosen. This means that all loading experiments were conducted on a particular body part of a living test person using a specifically constructed testing device.

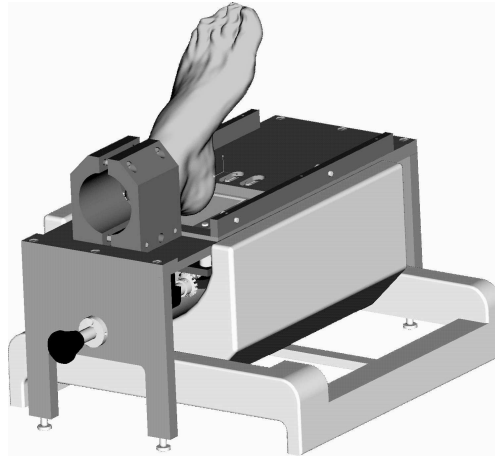


Fig. 2. Experimental device for loading body part

Figure 2 shows an experimental device for loading particular body parts with a mounted foot as an example of a body part. The foot is attached on this device by a cast sleeve on the upper face of it. Underneath of the foot there is a plate which can be moved towards the heel by a drive shaft. To record the reaction force, a transducer was integrated between the lower face of the plate and the spindle. This transducer was calibrated with standards weights. The displacement of the pressure plate was measured by a rotary encoder fixed on the drive shaft. The plate can be exchanged for an indenter as a test body. Two different body parts were tested. The heel with the plate as a test body and the calf with the indenter.

**Geometric measurement:** For grabbing the geometry of the loaded and unloaded body site, an imaging device was used. For this purpose the loading device was integrated into an MRI. First the mounted body part was measured in an unloaded condition. After this measurement was done, the load and displacement transducers were attached to the loading device. This body part was then loaded manually and force and displacement were recorded. When a predetermined load was applied, the sensors were detached and the deformed state was measured inside the MRI again. After finishing the second imaging process, the transducer was attached again and the loading process was applied reversibly.

**Load experiment with holding times:** Human soft tissue shows a combination of elastic and inelastic behavior. To separate these properties, a testing procedure proposed by (Van den Bogert and de Borst, 1994), successfully applied by (Hartmann et al., 2003) and (Lion, 1996) for rubber-like materials as well as (Schrodt et al., 2005) for polymeric soft foams. For the sake of distinguishing between elastic and viscoelastic load signals, such a stepwise loading and unloading regime was also applied here (see Figure 3 a). To minimise the load impact on the test person, the holding time at the termination points was one minute. Figure 3 b shows that the material reacts at the holding time with a relaxation while loading and a recovery while unloading. Apparently

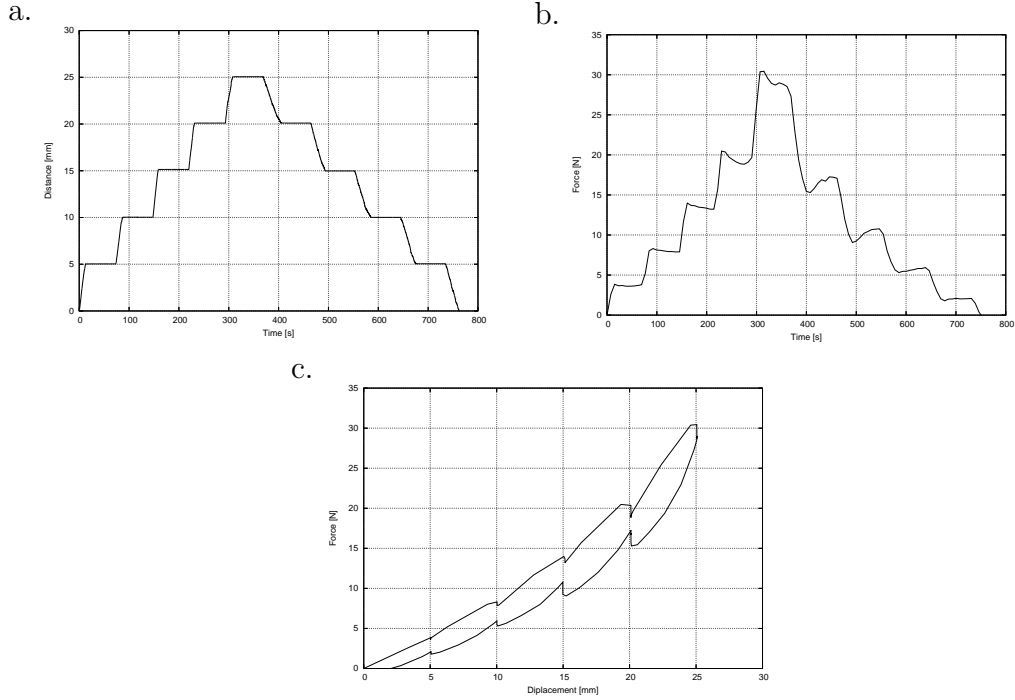


Fig. 3. Example of a loading regime for body parts (a. displacement vs. time, b. force vs. time and c. force vs. displacement)

the holding time is not sufficient to discriminate the elastic behavior from the inelastic. But the termination points indicate the range in which the elastic response of the material must be. Thus these points were taken as the experimental data for the parameter identification process described in section 6.

## 4 3D Reconstruction and Mesh Generation

The acquired image stacks from the experiments described in the previous section have to be used for a 3D reconstruction. This was performed by using 3D reconstruction software. The goal of this reconstruction was to obtain 3D surface models of different tissue types of the body sites. The chosen types were: bone, muscle and a mixed tissue type consisting of skin, fat and connective tissue. The reconstruction was done using 3D reconstruction software (MIMICS).

For this kind of classification, no automatic selection could be used because no uniform gray levels for the different tissue types were generated over all slices by the MRI device. Thus the areas of the different tissue types were selected manually slice by slice. Afterwards boundary layers for selected areas was automatically generated by the program. These boundary layers were linked together for all slices to finally build up a 3D surface of the selected tissue types (see Figure 4).

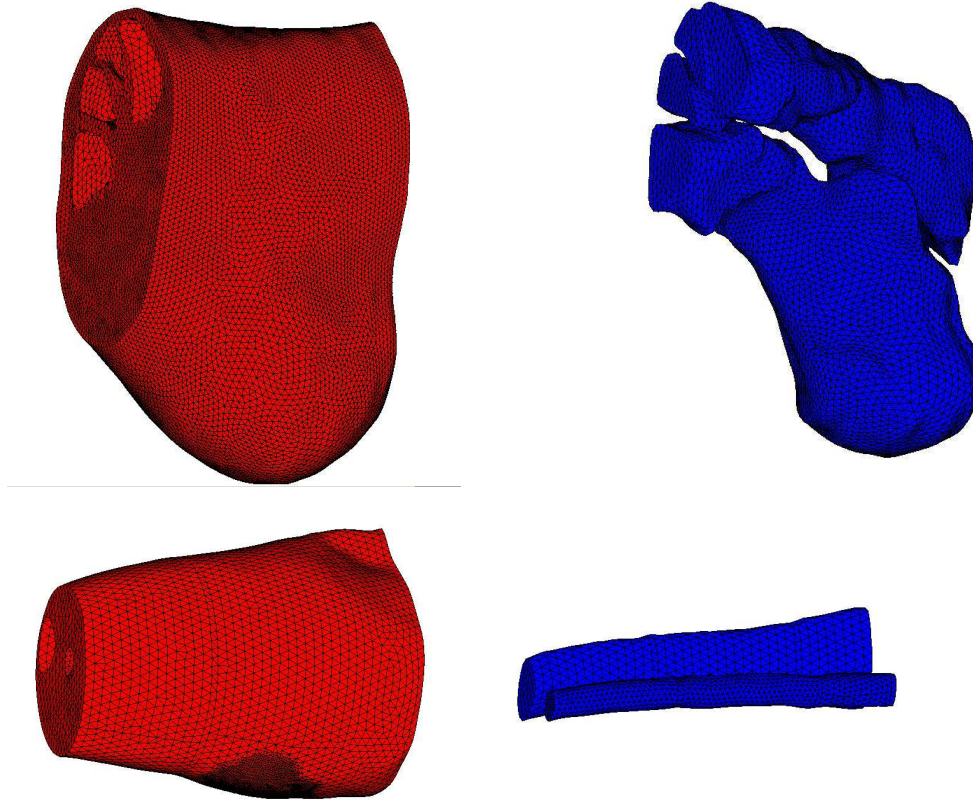


Fig. 4. 3D tetra mesh of the heel (top) and calf (bottom): left side soft tissue, right side bone

To generate a volume mesh of the different body sites a finite element tool (HYPERMESH) was used because in this case the mesh algorithm provided in MIMICS created an inadequate mesh. To generate a volume mesh for the different tissue types, two separate actions were necessary. First the surfaces of the tissue types were manually selected and then meshed using 2D elements (tria) using the automesh module. Starting from the 2D-element mesh of the surfaces the volume mesh of the tissue types was automatically created by the program with 3D elements (tetrahedral elements).

#### 4.1 Model

The system was solved with three dimensional first order tetrahedral elements (C3D4) in the ABAQUS standard FEA package (Version 6.4-1) in which the soft tissue was modeled as a hyperelastic model (see section 5) undergoing finite deformation, whereas the bone tissue was modeled by a linear elastic approach (HOOKE) because, at the applied loading, bone wouldn't react hyperelastically, so this simple approach is adequate.

Because the soft tissue at the chosen test site is dominated by one specific

tissue type (fat at the heel and muscle at the calf) the tissue at these sites were not subdivided into different tissue types. The pressure plate and the intender were generated as an analytical rigid with a reference node for calculating the resultant contact force and the corresponding displacements in loading direction. A constant friction coefficient of 0.75 was assumed between the test bodies and the surface of the test models. The body parts at the test sites, which were mounted on the experimental device were modeled suppressing all degrees of freedoms at each surface node.

## 5 Constitutive Equation

According to the results of the in vivo empirical analysis the human tissue materials of the fat-muscle compounds show a slightly compressible viscoelastic material behavior (see Figure 3). To describe such phenomena, normally a viscoelastic constitutive equation is adopted. In general, viscoelastic models decompose the total stress tensor  $\mathbf{S}$  into an (elastic) equilibrium stress part  $\mathbf{S}_G$  and an overstress part  $\mathbf{S}_{ov}$  representing the memory property of the material. Thus the stress tensor can be written as  $\mathbf{S} = \mathbf{S}_G + \mathbf{S}_{ov}$  (see Hartmann (2001)). This study will exclusively deal with the elastic properties of human tissue according to the empirically attained stress-strain curves of the termination points after a distinct holding time (see section 3). For such a description, constitutive equations for hyperelasticity are permissible (Hartmann, 2001). For the sake of simplicity the index G in the above formula will be left out of the further discussion.

Hyperelastic materials represent a subset of the (CAUCHY-) elastic materials characterized by an elastic potential (strain energy function). The stress tensor can be generated by the derivative of the energy function with regard to the strain tensor. The basis therefore is the balance of mechanical energy.

$$\dot{w} = J \mathbf{S} \cdot \cdot \mathbf{D} \quad \text{with} \quad J = \det \mathbf{F} \quad (1)$$

where  $w$  is the strain energy function,  $\mathbf{F}$  the deformation gradient,  $\mathbf{S}$  the CAUCHY stress tensor and  $\mathbf{D}$  the strain rate tensor which reads:

$$\mathbf{D} = \frac{1}{2} \mathbf{F}^{-T} \cdot \dot{\mathbf{C}} \cdot \mathbf{F}^{-1} \quad (2)$$

with the right CAUCHY-GREEN tensor  $\mathbf{C}$  (a dot above the symbol means the material time derivative). Due to the principles of Rational Mechanics (causality, determinism, equipresence, objectivity, neighborhood)  $w$  has to be

a scalar-valued non-negative tensor function of the right stretch tensor  $\mathbf{U}$  respectively the right CAUCHY-GREEN tensor, thus that:

$$w = w(\mathbf{F}) = w(\mathbf{U}) = w(\mathbf{C}) = \begin{cases} > 0, & \text{for } \mathbf{C} \neq \mathbf{I} \\ = 0, & \text{for } \mathbf{C} = \mathbf{I} \end{cases} \quad (3)$$

According to (3) in the undeformed state (reference configuration  $\mathbf{C} = \mathbf{I}$ ) the strain energy  $w$  is always zero and for the deformed state (current configuration  $\mathbf{C} \neq \mathbf{I}$ ) the strain energy always has to be non-negative ( $w > 0$ ). Inserting (3) into (1) by regarding (2) results in the most general structure of constitutive equation for non linear, hyperelastic, anisotropic material behavior (Green and Adkins, 1970).

$$\mathbf{S} = 2 J^{-1} \mathbf{F} \cdot \frac{\partial w(\mathbf{C})}{\partial \mathbf{C}} \cdot \mathbf{F}^T \quad (4)$$

For a first approximation of the continuum mechanical modeling of the important human soft tissues in the heel and calf region a hyperelastic model of OGDEN type for slightly compressible isotropic materials given in ABAQUS was used Hibbitt et al. (2000). Bones were modeled by a linear elastic approach (HOOKEian behavior). In the area of compressible hyperelastic materials it is useful to perform a multiplicative decomposition of the deformation gradient  $\mathbf{F}$  into a volume changing (dilatational) part  $\bar{\mathbf{F}}$  and a volume preserving (distortional) part  $J^{\frac{1}{3}}\mathbf{I}$  so that (see e.g. Lee (1969))

$$\mathbf{F} = (J^{\frac{1}{3}}\mathbf{I} \cdot \bar{\mathbf{F}}) \equiv J^{\frac{1}{3}}\bar{\mathbf{F}} \quad (5)$$

With (5) one gets the relation between the modified principal stretches (deviatoric principal stretches)  $\bar{\lambda}_i$  and the eigenvalues  $\lambda_i$  (principal stretches) of the right stretch tensor  $\mathbf{U}$

$$\bar{\lambda}_i = J^{-\frac{1}{3}} \lambda_i \quad (i = 1, 2, 3) \quad \text{with } J := \det \mathbf{F} \quad (6)$$

With regard to (6) the decomposed strain energy function leads to (Ogden, 1972)

$$w = \sum_{k=1}^N 2 \frac{\mu_k}{\alpha_k^2} \left( \bar{\lambda}_1^{\alpha_k} + \bar{\lambda}_2^{\alpha_k} + \bar{\lambda}_3^{\alpha_k} - 3 \right) + f(J) \quad (7)$$

whereby  $\alpha_k$  and  $\mu_k$  are  $3N$  material coefficients and  $f(J)$  is the volumetric elastic function. For slightly compressible materials  $f(J)$  for instance, is given by Hibbitt et al. (2000) in the form:

$$f(J) := \sum_{k=1}^n \frac{1}{D_k} (J-1)^{2k} \quad (8)$$

where  $D_k$  are additional material parameters. The initial shear and bulk moduli  $\mu_0$  and  $K_0$  are given by (Hibbitt et al., 2000):

$$\mu_0 := \sum_{i=1}^N \mu_i \quad K_0 = 2 D_1^{-1} \quad (9)$$

Additionally the following relation between the POISSON ratio  $\nu$  and the initial shear and bulk modulus holds:

$$\nu = \frac{3 K_0 / (\mu_0 - 2)}{6 K_0 / (\mu_0 + 2)} \quad (10)$$

Together with (9) and (10) one can follow:

$$D_1 = \frac{3}{\mu_0} \frac{1 - 2\nu}{1 + \nu} \quad (11)$$

The constitutive equation for non linear, hyperelastic, anisotropic material behavior for the CAUCHY stress tensor in spectral form reads (Ogden, 1972):

$$\mathbf{S} = J^{-1} \sum_{i=3}^1 \lambda_i \frac{\partial w}{\partial \lambda_i} \mathbf{n}_i \mathbf{n}_i \quad \text{with} \quad J = \lambda_1 \lambda_2 \lambda_3 \quad (12)$$

with the eigenvectors  $\mathbf{n}_i$  of the left stretch tensor  $\mathbf{V}$ .

With regard to (7), (8) and (12) one obeys the following final constitutive equation for slightly compressible hyperelastic materials in terms of the principal stretches versus the modified principal stretches (for  $J$  see (12)):

$$\begin{aligned}
\mathbf{S} &= 2 J^{-1} \sum_{i=1}^3 \sum_{k=1}^N \left[ \frac{\mu_k}{\alpha_k} J^{-\frac{\alpha_k}{3}} \left( \lambda_i^{\alpha_k} - \frac{1}{3} \sum_{j=1}^3 \lambda_j^{\alpha_k} \right) + \frac{k}{D_k} J (J-1)^{2k-1} \right] \mathbf{n}_i \mathbf{n}_i \\
&= 2 J^{-1} \sum_{i=1}^3 \sum_{k=1}^N \left[ \frac{\mu_k}{\alpha_k} \left( \bar{\lambda}_i^{\alpha_k} - \frac{1}{3} \sum_{j=1}^3 \bar{\lambda}_j^{\alpha_k} \right) + \frac{k}{D_k} J (J-1)^{2k-1} \right] \mathbf{n}_i \mathbf{n}_i
\end{aligned} \tag{13}$$

## 6 Optimization

The basic goal is to describe the elastic properties of the material by constitutive equations, so that these functions represent the empirical data in an appropriate way. This is obtained by using a quality function  $\Phi$  of the following form:

$$\chi^2 := \sum_{i=1}^n [f(h; \alpha_1, \dots, \alpha_N) - f_i(h_i)]^2 \stackrel{!}{=} \min \tag{14}$$

where  $f(h; \alpha_1, \dots, \alpha_N)$  is the model with  $h$  the independent variable, the  $\alpha_1, \dots, \alpha_N$  are arbitrary model parameters and  $f_i$  and  $h_i$  are the measured values.

In this particular case the model is the constitutive equation (13)  $\mu_i, \alpha_i$  and  $D_i$  are the model parameters. The values for the  $f_i$  and  $h_i$  were taken from the measured data of the loading test described in the section 3.

**Optimization routines:** Finding the minimum of the quality function (14) is usually done using an optimization routine. Because most of the parameters within the constitutive equations appear in a non linear way, for minimizing the quality function (14) a non linear optimization routine has to be used for this purpose. To solve the boundary problem within the quality function is only possible in a numerical way. This is done using an FE tool (ABAQUS). Because this is a rather time consuming process a *Hill Climbing* strategy (due to the classification of Schwefel (1995)) called *Simplex Strategy* by Nelder and Mead (1969) was chosen.

## 7 Results

In Figure 5 the results of the load experiments for the heel and the calf are shown. Because of the steepness of the signal progression for the heel, less holding points could be set compared to the calf.

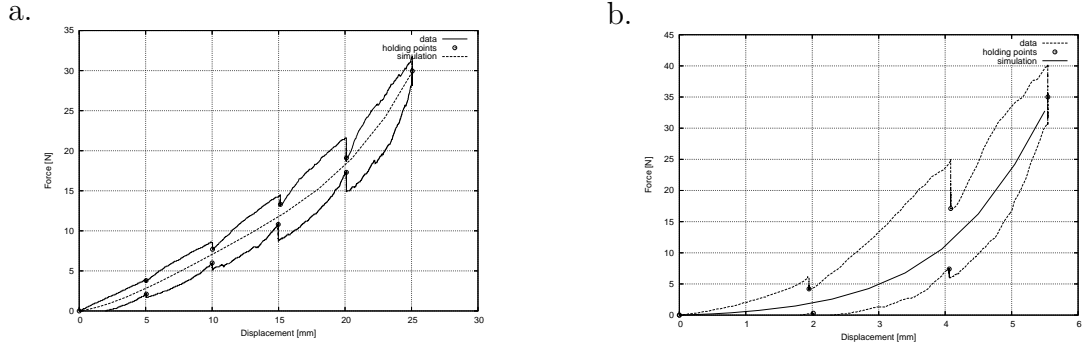


Fig. 5. Results of the loading experiments including the FE simulation (a. calf, b. heel).

Table 1  
Parameter set

| body part | $\mu [MPa]$   | $\alpha$      | $\chi^2$ |
|-----------|---------------|---------------|----------|
| calf      | 0.8335823E-02 | 0.7801210E+01 | 4.393327 |
| heel      | 0.9195020E-02 | 0.2998462E+02 | 6.286381 |

Table 1 shows the optimized parameters for the constitutive equation (13) used for the FE simulation in figure 5. The material parameter  $D$  in equation (13) is missing in table 1. To allow a weak compressibility within the constitutive equation (13) according to the manual of the FE tool (Hibbitt et al., 2000) it is proposed to use a 'Poisson ratio' of  $\nu = .495$ . The relation of the compression parameter  $D$  and the 'Passon ratio' is given in (11).

Apparently the FE simulations in figure 5 lie within the range given by the holding points. This indicates that the simulations can be carried out with the proposed constitutive model of section 5 and most probably represents the remaining elasticity of the viscoelastic material behavior. Also the difference between the several soft tissues can be seen in the results. The heel dominated by fat tissue shows a much more rigid material response to loading compared to the calf dominated by muscle tissue.

Finally the optimization process was only successful by implementing a weak compressibility in the FE simulation. This reflects the water permeability of the soft tissues.

## 8 Discussion and Conclusion

As one can see in figure 1 the water charge effects the mechanical response to external loading substantially. Thus test specimens taken from the tissue for the sake of having a simple geometry will probably destroy the cover. But even when the cover is not destroyed, the filling state of the structure is difficult to

control and to adjust at the level found inside of a body.

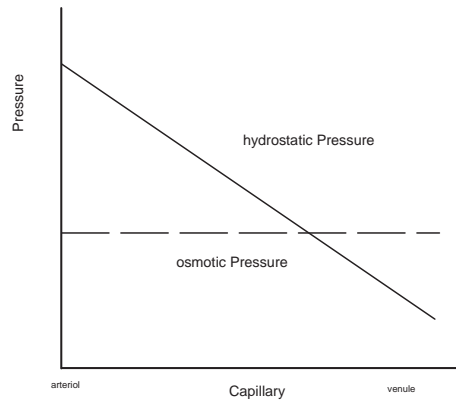


Fig. 6. Scheme of the pressure conditions within the capillary blood vessels

In figure 6 the antagonism between the hydrostatic blood pressure and the osmotic pressure in the tissue is given. At the site of the arterioles the high blood pressure is responsible for pressing water into the tissue. Because of the high hydraulic resistance of the capillaries, the hydrostatic pressure drops and the osmotic pressure is responsible for retrieving a certain amount of water into the blood vessels. The osmotic pressure is dominated by the amount of blood proteins and thus is controlled by the individual organism itself showing a great diversity from healthy to pathological states like hypertension or hunger oedemas. So only a living organism guarantees a constant hydrogenation level by the interaction of osmotic active particles inside the blood with the blood pressure generated by the heart and the excretion of surplus water by the kidneys. Due to this regulation process, the derived parameters are only valid for the individual with whom the experiments were carried out and his current hydraulic state. Whereas the variability for healthy individuals probably will be smaller than the variability between a healthy and an unhealthy state.

Moreover this hydraulic regulation process of a healthy person seems to be responsible for a filling condition of the tissue which is close to the situation shown on the right side of figure 1.

In this analysis only the elastic properties of soft tissues were determined. Using this method also allows to determine the visco elastic properties of the tissue. In the case of the muscle there is a superposition between the elastic properties of the tissue and the muscle contraction. This phenomenon causes additional uncertainties in the parameters, because no muscle immobilization was applied during the measurements.

Finally, it is not surprising that to gain satisfactory results by the parameter optimization process, weak compressibility has to be used for the FE simulation. This reflects the fact that the hydraulic state of the tissue in a compression test is shifted because the test force acts in the opposite direction to the

osmotic pressure. Thus the tissue loses water and its volume shrinks during the test.

## References

- Daly, S., Prendergast, P. J., Dolan, F., Lee, T. C., 2000. Use of finite element analysis to simulate the hyperelastic behaviour of cardiovascular tissue. In: Prendergast, P. J., Lee, T. C., Carr, A. J. (Eds.), Proceedings of the 12th Conference of the European Society of Biomechanics. Royal Academy of Medicine in Ireland, p. 242.
- Green, A. E., Adkins, J. E., 1970. Large Elastic Deformation, 2nd Edition. Oxford University Press, Oxford.
- Hartmann, S., 2001. Numerical studies on the identification of material parameters of rivlin's hyperelasticity using tension-torsion tests. *Acta Mechanica*.
- Hartmann, S., Tschöpe, T., Schreiber, L., Haupt, P., 2003. Finite deformations of a carbon-black-filled rubber, experiment, optical measurement and material parameter identification using finite elements. *European Journal of Mechanics A/Solids* 22.
- Hibbitt, Karlsson, Sorensen, 2000. ABAQUS, Theory Manual, 6th Edition. Abacom Software GmbH.
- Lee, E. H., 1969. Elastic-plastic deformation at finite strains. *Journal of Applied Mechanics* 36, 1–6.
- Lion, A., 1996. A constitutive model of carbon black filled rubber: Experimental investigations and mathematical representation. *Continuum Mech.* 8.
- Maenhout, M., Hesselink, M. K. C., Oomens, C. W. J., Drost, M. R., 2000. Muscle deformation measurements to validate a 2-d-continuum model of muscle. In: Prendergast, P. J., Lee, T. C., Carr, A. J. (Eds.), Proceedings of the 12th Conference of the European Society of Biomechanics. Royal Academy of Medicine in Ireland, p. 249.
- Miller, J. E., Duncan, N. A., Baroud, G., 2002. Material properties of the human calcaneal fat pad in compression: experiment and theory. *Journal of Biomechanics* 35, 1523–31.
- Miller, K., Chinzei, K., 1997. Constitutive modelling of brain tissue: Experiment and theory. *Journal of Biomechanics* 30, 1115–21.
- Moes, N., Horvath, 2002. Finite element model of the human body: geometry and non-linear material properties. In: Proceeding of the TMCE, Wuhan.
- Nelder, J. A., Mead, R., 1969. A simplex method for function minimization. *Comp. J.* 7, 308–313.
- Ogden, R. W., 1972. Large deformations isotropic elasticity –on the correlation of theory and experiment for incompressible rubberlike solids. In: Proceedings of the Royal Society of London, Series A. Vol. 326. pp. 565–584.
- Palevski, A., Glaich, I., Linder-Ganz, E., Gefen, A., 2006. Stress relaxation of porcine gluteus muscle subjected to sudden traverse deformation as related to pressure sore modeling. *Journal of Biomechanical Engineering*, 782–7.
- Sacks, M. S., 2000. Biaxial mechanical evaluation of planar biological materials. *Journal of Elasticity* 61, 199–246.
- Samani, A., Plewes, D., 2004. A method to measure the hyperelastic param-

- eters of ex vivo breast tissue samples. *Physics in Medicine and Biology* 49, 4395–4405.
- Schrodt, M., Benderoth, G., Kühhorn, A., Silber, G., 2005. Hyperelastic description of polymer soft foams at finite deformations. *Technische Mechanik* 25 (3-4), 162–73.
- Schwefel, H. P., 1995. *Evolution and Optimum Seeking*. Wiley & Sons, New York.
- Van den Bogert, P. A. J., de Borst, R., 1994. On the behaviour of rubberlike materials in compression and shear. *Arch. Appl. Mech.* 64.